TEXTURAL EVOLUTION IN TI-RICH AND NI-RICH NI-TI SHAPE MEMORY ALLOYS SUBMITTED TO THERMOMECHANICAL TREATMENT WITH MARFORMING STEPS[1]

Andersan dos Santos Paula[2]
Christian Mariani Lucas dos Santos[3]
João Heitor Paulo Godinho Canejo[4]
Karimbi Koosapa Mahesh[5]
Francisco Manuel Braz Fernandes[6]
Carlos Sérgio da Costa Viana[7]

Abstract
In alloys with shape memory effect (SME) and superelasticity (SE), the crystallographic texture can be an interesting factor promoting anisotropic characteristics of physical and mechanical properties of an electrical and/or mechanical component during the phase transformation. In this study, two Ni-Ti alloys, one Ni-rich and another Ti-rich, were submitted to a marforming thermomechanical treatment (30% thickness reduction in the plate) with a previous and post heat treatment at 500ºC for 30 minutes followed by water quenching. The martensite (B19') and austenite (B2) textures were measured by X-ray diffraction (XRD). Differential scanning calorimetric (DSC), electrical resistivity (ER) and XRD were employed to detect and identify the transformation temperatures and the respective phases (B19', R-phase and B2). In the as-received condition, Ti-rich and Ni-rich NiTi alloys exhibited R-phase formation previous to the B19' transformation on cooling and B2 transformation on heating. The direct and reverse transformations are strongly affected by the thermomechanical treatment, with SME suppressed due to the high level of deformation during the marforming Further, R-phase transformation is found to be absent, giving rise to one step (B2↔B19') phase transformation, when heat treated at 500ºC is probably due to the completion of recrystallization process. The thermomechanical treatment developed a texture formed by α-fibre II (<110>||DL, {110}<110>B2 and {111}<110>B2) and {001}<110>B2 texture component that is part of α-fibre I (<110>||DL, {001}<110>B2, {112}<110>B2 and {111}<110>B2).
Key-words: NiTi shape memory alloy; Thermomechanical treatment; Marforming; Texture.

EVOLUÇÃO TEXTURAL EM LIGAS COM MEMÓRIA DE FORMA DE NI-TI RICAS EM TI E EM NI SUBMETIDAS A TRATAMENTOS TERMOMECÂNICOS COM ETAPA DE MARFORMING

Resumo
Nas ligas com efeito de memória de forma (EMF) e superelasticidade (SE), a textura pode ser um fator interessante conduzindo a características anisótropas nas propriedades físicas e mecânicas de um dado componente elétrico e/ou mecânico durante a transformação de fase. Neste estudo, duas ligas de Ni-Ti, uma rica em Ni e outra rica em Ti, foram submetidas a um tratamento termomecânico de marforming (30% de redução na espessura da chapa) com um tratamento térmico prévio e outro posterior a 500ºC com 30 min de manutenção e têmpera em água. As texturas da martensita (B19') e austenita (B2) foram medidas qualitativamente por difração de raios-X (DRX). Por calorimetria diferencial de varredura (DSC), resistividade elétrica (RE) e DRX foram detectadas e identificadas as temperaturas de transformação e as fases (B19', fase-R e B2). As ligas de Ni-Ti rica em Ti e rica em Ni na condição como recebida apresentam formação de fase-R prévia às transformações em B19' no resfriamento e em B2 no aquecimento. As transformações direta e inversa são fortemente afetadas pelo tratamento termomecânico, com supressão do EMF devido ao alto grau de deformação imposto pelo marforming e eliminação da formação de fase-R devido à completa recristalização pelo tratamento térmico a 500ºC que promove as transformações direta e inversa em uma etapa (B2↔B19'). O tratamento termomecânico desenvolve uma textura composta pela textura de Fibra α-II (<110>||DL, {110}<110>B2 e {111}<110>B2) e a componente {001}<110>B2 pertencente à textura de Fibra α-I (<110>||DL, {001}<110>B2, {112}<110>B2 e {111}<110>B2).
Palavras-chave: Liga com memória de forma de Ni-Ti; Tratamento termomecânico; Marforming; Textura.

---

[1] *Technical contibution to 62nd ABM - International Annual Congress, July 23rd to 27th, 2007, Vitória - ES – Brazil*
[2] *D.Sc. Researcher at Divisão de Metrologia de Materiais, INMETRO – Brazil*
[3] *D.Sc. Professor at Faculdade do Centro Leste, UCL – Brazil*
[4] *Ph.D Student at Faculdade de Ciências e Tecnologia, UNL – Portugal*
[5] *Ph.D Fellowship at Faculdade de Ciências e Tecnologia, UNL – Portugal*
[6] *D.Sc. Professor at Faculdade de Ciências e Tecnologia, UNL – Portugal*
[7] *Ph.D. Professor at Escola de Engenharia Industrial Metalúrgica de Volta Redonda, UFF – Brazil*

1 INTRODUCTION

The shape memory alloys (SMA) are very sensitive to changes in the chemical composition and thermal and/or mechanical treatments. The phase transformations responsible for the shape memory effect (SME) in the Ni-Ti SMA are greatly affected by thermal treatments.[1-3] The influence of cold work, annealing and precipitation kinetics during aging on martensitic transformation in the Ni-Ti alloy have been studied by many researchers.[4-6]

In most polycrystalline materials, crystal orientations are present in a definite pattern and a propensity for this occurrence is caused initially during crystallization from the melt or amorphous solid state and subsequently by thermomechanical processes. This tendency is known as preferred orientation or, more concisely, the texture. Many material properties (Young's modulus, Poisson's ratio, strength, ductility, toughness, electrical conductivity etc.) depend on the average texture of a material.

Several studies are dedicated to the influence of texture on the thermomechanical response of the SMAs, mainly using in-situ neutron radiation to follow up the structural evolution.[7] Thermal cycling, rolling or drawing are found to develop specific texture in metals and alloys. They result in different anisotropy characteristics (mechanical, electrical and magnetic behaviour). NiTi SMAs are also sensitive to these effects. The texture is found to give rise to anisotropy in transformation recovery strain.[8] NiTi SMA in austenitic field has a bcc type texture:[9,10] α-fibre I <110>||RD ({001}<112>-{112}<110>-{111}<110>), α-fibre II <110>||RD ({111}<110>-{110}<110>), γ-fibre <111>||ND ({111}<110>-{111}<112>), and η-fibre <100>||RD ({001}<100>-{011}<100>). The calculated lattice correspondence between parent phase and martensite using the Miyazaki's correspondence variant notation [10], where the (110)[$1\bar{1}0$] parent phase variant gives rise to {111}<211> and {002}<002> martensite variants; and the (111)[$1\bar{1}0$] parent phase variant gives rise to {210}<211> and {210}<002> martensite variants.

In the present work, the cold rolling (marforming) on the texture was studied in two Ni-Ti alloys, one Ti-rich (Ni-51.0at.%Ti) with SME above room temperature and another Ni-rich (50.8at.%Ni-Ti) superelastic at room temperature. The phase transformations were analyzed by differential scanning calorimetry (DSC) and electrical resistivity (ER).

2 MATERIALS AND METHODS

The materials in study are two Ni-Ti, one Ti-rich (49.0at.%Ni-51.0at.%Ti, according to SEM/EDS and thickness 2.00 mm) that exhibit shape memory characteristics above room temperature (T_{room}) and another Ni-rich (50.8at.%Ni-49.2at.%Ti, according to supplier and thickness 1.00 mm) that exhibit superelastic characteristic (SE) at T_{room}.

The Ni-Ti alloys were supplied by Memory-Metalle GmbH, Germany (www.memory-metalle.de). According to supplier information, the Ni-Ti alloys were melted in a vacuum induction melting furnace under argon atmosphere, using compact graphite crucibles.

- Thermomechanical Treatment

The thermomechanical treatment consists of three steps (Figure 1):

- in the first step, a previous thermal treatment in air, where the samples

were introduced in the furnace at 500ºC during 30 minutes and water quenched, in order to recrystallize the material prior to cold-rolling,

- in the second step, the sample is subjected to a marforming (cold rolling with 30% thickness reduction),
- in the third step a post thermal treatment in air, where the samples entered the furnace at 500ºC and, after 30 minutes soaking, were water quenched.

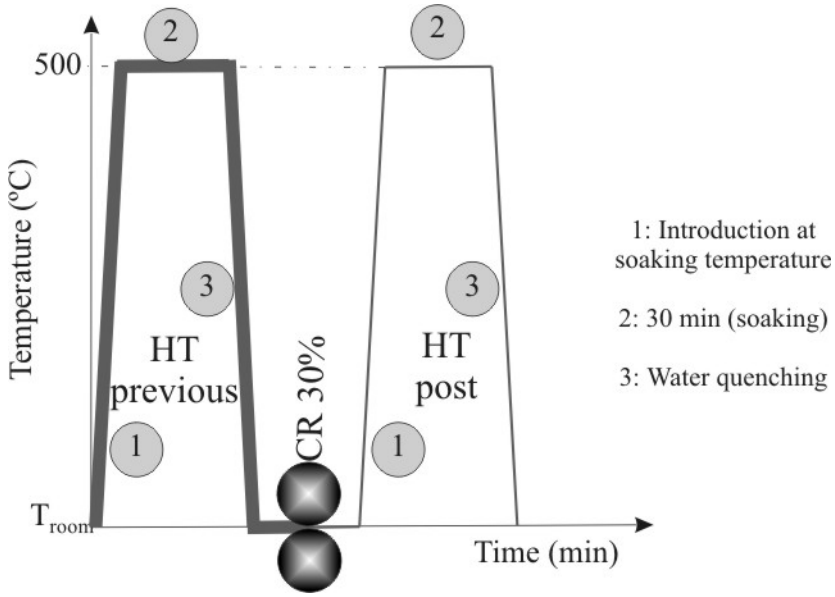

Figure 1 – Schematic diagram for thermomechanical treatment.

- Thermal and Structural Characterization

XRD analysis was performed using a Bruker diffractometer (30 kV/100 mA, rotating anode, CuKα radiation) with conventional θ/2θ scanning and texture analysis, both in the temperature range from T_{room} to 150ºC. The rolling direction (RD) was kept aligned in φ = 0º and transversal direction (TD) in φ = 90º.

Samples with a mass ranging from 40 to 50 mg were cut for DSC analysis (SETARAM DSC92). The thermal cycle for the DSC comprised (i) heating up to 180ºC, (ii) holding for 360 s and (iii) subsequent cooling down to -30ºC with heating and cooling rates of 7.5ºC/min.

ER characterisation has been performed on a home made four-probe set up, which was immersed, together with the sample, in a silicone oil bath with temperature control. It consists of a block of 4 copper rods with wedge-shaped tips. The position of the rods as well as the pressure that they exert on the test specimen is individually controlled. A controllable power supply is used to apply the current (1600 mA) into the test specimen. Data acquisition board (National Instruments, USA) with a precision better than 1 μV has been used to send the signal to a PC. Samples have been scanned in the temperature range from -20 to 150ºC.

3 RESULTS

Figure 2 shows the thermal characterisations with complete cycles by DSC for SME and SE alloys, in the following conditions: (i) as-received (AR), (ii) heat treated in air at 500ºC followed by water quenching (HT), (iii) HT and subsequent cold rolling (marforming) followed by HT (HT+CR+HT). In the Figure 2a on cooling is shown two

peaks exothermic overlapped (B2→R; B2→B19' and R→B19') obtained by deconvolution process with CGAS function using "Peak Fitting – Origin 7 software)".[11] Figure 3 shows typical thermal characterisation curves by electric resistivity (ER) for the transformation sequences observed in the samples in study.

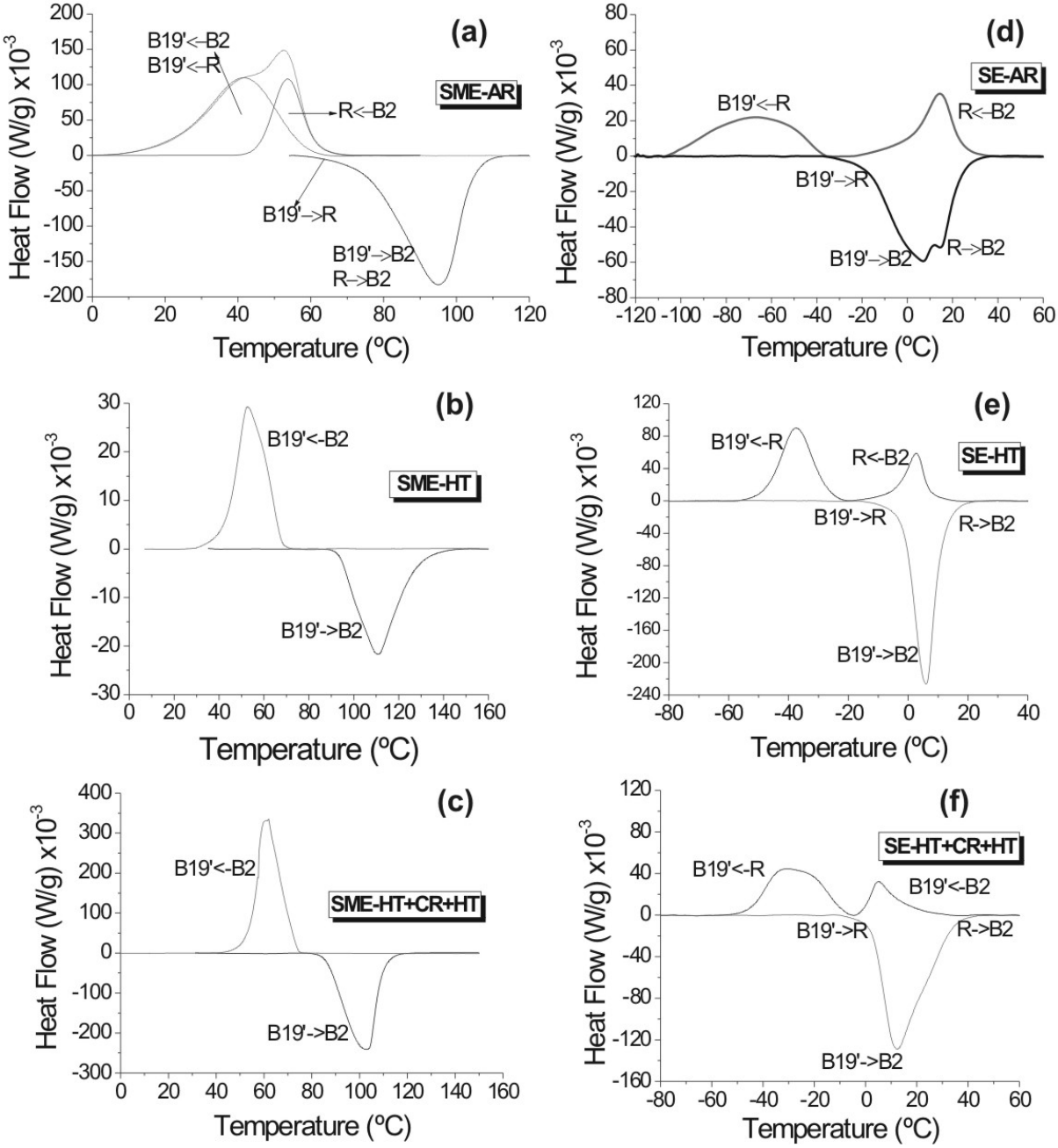

Figure 2 – DSC curves: (a) SME-AR; (b) SME-HT; (c) SME-HT+CR+HT; (d) SE-AR; (e) SE-HT; and (f) SE-HT+CR+HT.

The transformation temperatures obtained from DSC analysis and transformation sequences observed by ER are given in Table 1. These values were taken from the kinetics curves calculated by integration of the DSC peaks.[11]

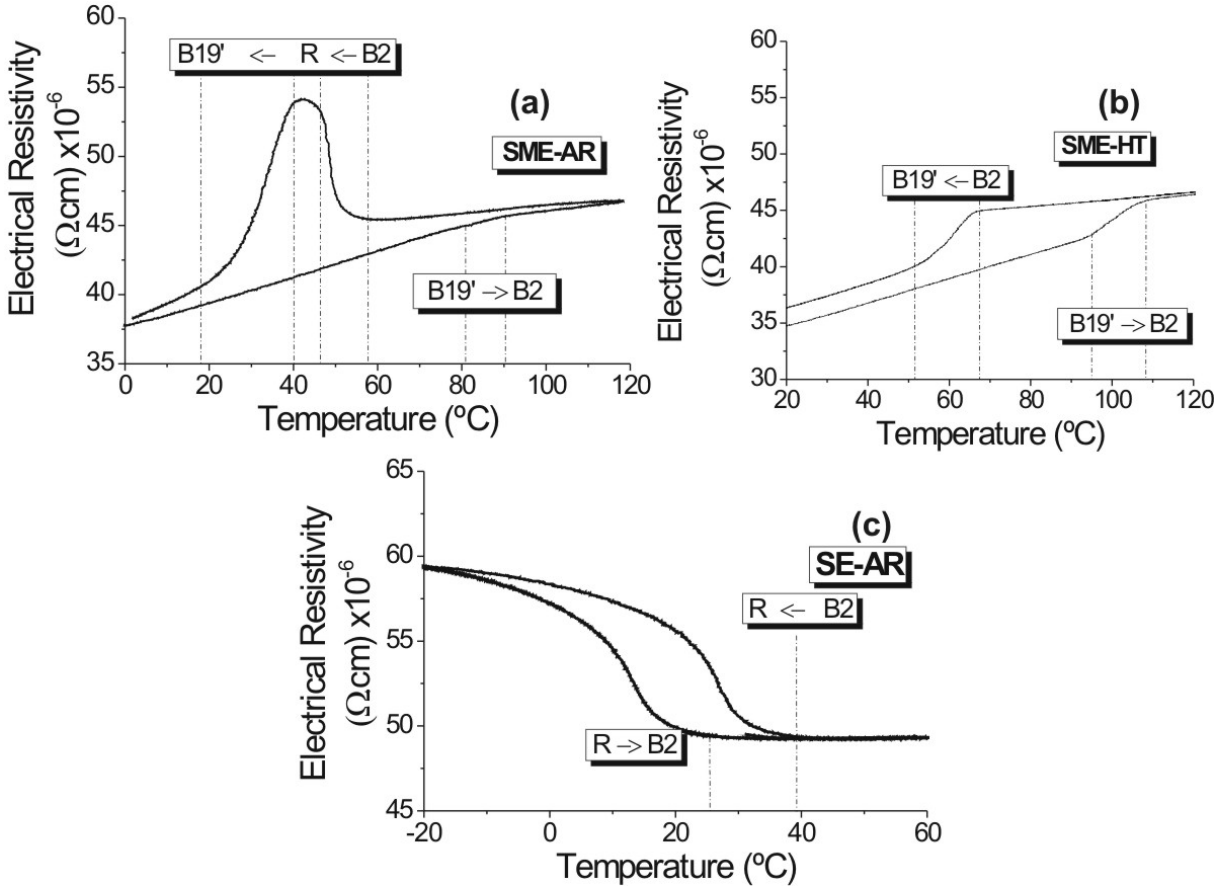

Figure 3 – Typical behaviour on ER tests observed in samples under study: (a) multiple-steps on cooling and one step on heating, e.g. SME-AR; (b) one step on cooling and on heating, e.g. SME-HT; and (c) B2→R in two-steps transformation on cooling interrupted above M_s'', e.g. SE-AR.

Table 1 – Sequence and transformation temperatures extracted from DSC and ER analyses.

Structural Condition	Sequences and Transformations Temperatures (ºC)											
	Cooling						Heating					
	B2→R		B2→B19'		R→B19'		B19'→R		B19'→B2		R→B2	
	R_{sc}	R_{fc}	M_s'	M_f'	M_s''	M_f''	R_{sh}	R_{fh}	A_s'	A_f'	A_s''	A_f''
Ti-rich Ni-Ti alloy (SME)												
AR	64.9	44.3	58.7	*	*	13.5	66.8	*	*	*	*	106.6
HT	-	-	67.0	35.6	-	-	-	-	94.3	136.0	-	-
HT+CR+HT	-	-	72.6	48.7	-	-	-	-	85.6	112.7	-	-
Ni-rich Ni-Ti alloy (SE)												
AR	29.6	-16.0	-	-	-40.4	-100.8	-30.6	*	*	*	1.9	27.9
TT	11.7	-13.9	-	-	-24.7	-51.6	-8.0	*	*	*	*	16.6
HT+CR+HT	27.9	-1.4	-	-	-9.6	-46.9	-1.7	*	*	*	*	36.1

A, R and M refer to the Austenite, Rhombohedral and Martensite phases, respectively. The subscripts s and f refer to the start (1% phase formed) and finish (99% phase formed) temperatures of phase transformations. (-) not detected. (*) identified only by ER.

Figures 4 and 5 show the pole figures, $(11\bar{1})_{B19'}$ and $(110)_{B2}$, for SME and SE alloys, respectively, in the following conditions: AR, HT and HT+CR+HT.

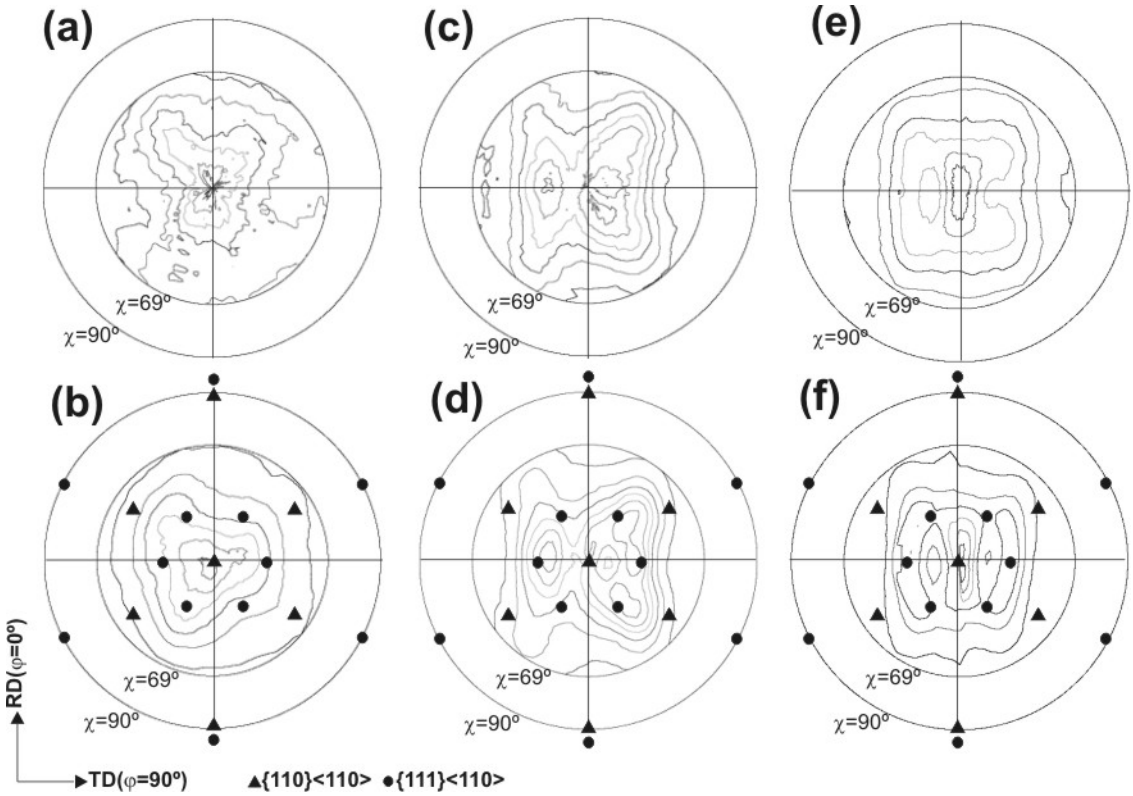

Figure 4 – Pole Figure of Ti-rich Ni-Ti alloy (SME): (a) AR in $(11\bar{1})_{B19'}$, (b) AR in $(110)_{B2}$, (c) HT in $(11\bar{1})_{B19'}$, (d) HT in $(110)_{B2}$, (e) HT+CR+HT in $(11\bar{1})_{B19'}$, and (f) HT+CR+HT in $(110)_{B2}$.

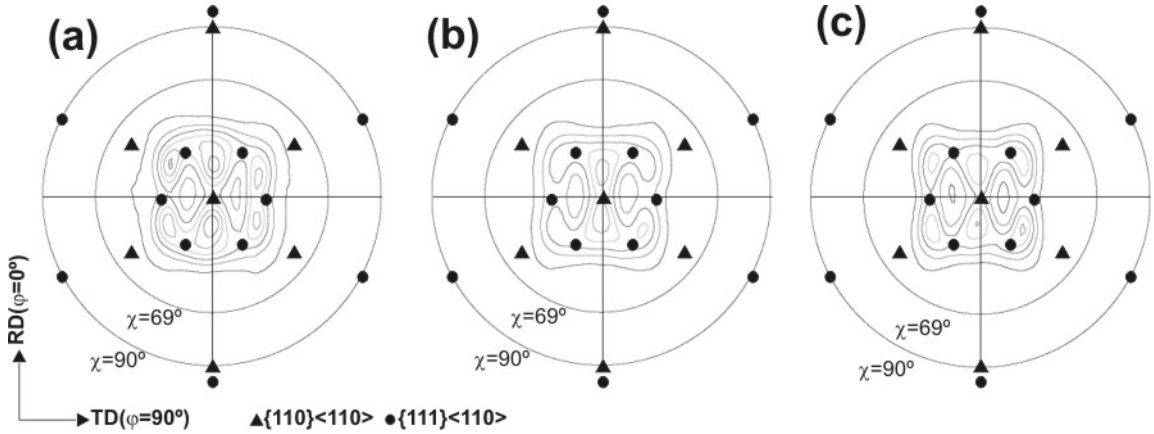

Figure 5 – Pole Figure $(110)_{B2}$ for Ni-rich Ni-Ti alloy (SE): (a) AR, (b) HT, and (c) HT+CR+HT.

4 DISCUSSION

From Table 1 and Figures 1a and 2a, it is clear that in (SME-AR) sample the phase transformations occur in multiple steps during cooling and heating (B2↔R; B2↔B19'; R↔B19'). In this case, when martensite transformation starts, R-phase transformation is not yet finished in another B2 matrix region. This may be due to the fact that the energy to start the B2→B19' in some B2 matrix regions is higher than that required for B2→R transformation.[12,13,17] For the heat treatment at 500ºC (HT – Table 1 and Figures 2b and 3b) in (AR) condition and after cold rolling (HT+CR – Table 1 and Figure 2c) for the SME alloy, it was found that R-phase transformation completely disappears, resulting in a one step transformation (B2→B19') on heating and on cooling.[12,13,17] On the other hand, (SE-AR) sample presents the phase

transformation in two steps during cooling (B2→R→B19') and multiple steps during heating (B19'→R; B19'→B2; R→B2),[17,18] is shown in Table 1 and Figures 2d and 3c. In this case, when martensite transformation starts during cooling, R-phase transformation is finished. This may be due to the fact that the energy to start the B2→B19' in B2 matrix is higher than that required for B2→R transformation; then, B2→B19' does not occur. For the heat treatment at 500ºC (HT) in (AR) condition and after cold rolling (HT+CR) of the SE alloy, it was found that R_s decreases and R_f increases, whether M_s and M_f increase.[18]

From Figure 4 a textural evolution is clearly observed by modifications in texture components in the SME alloy due to thermal and mechanical treatment:[14-17]

- AR condition (Figure 4a) for B19': central components associated with the variants 1:$(11\bar{1})[2\bar{1}1]_{B19'}$ and 4:$(11\bar{1})[\bar{2}1\bar{1}]_{B19'}$ corresponding to {110}<110>$_{B2}$.
- AR condition (Figure 4b) for B2: central component associated with texture component (110)[110]$_{B2}$, with RD in <110>.
- HT condition (Figure 4c) for B19': central components associated with the variants 1:$(11\bar{1})[2\bar{1}1]_{B19'}$ and 4:$(11\bar{1})[\bar{2}1\bar{1}]_{B19'}$ corresponding to {110}<110>$_{B2}$ and other variants 3:$(120)[\bar{2}11]_{B19'}$ and 5:$(120)[00\bar{2}]_{B19'}$ close to χ = 33º corresponding to {111}<110>$_{B2}$.
- HT condition (Figure 4d) for B2: central components associated with texture component (110)[110]$_{B2}$ and other components {111}<110>$_{B2}$ close to χ = 35º, with RD in <110>.
- HT+CR+HT condition (Figure 4e) for B19': strong central components associated with the variants 1:$(11\bar{1})[2\bar{1}1]_{B19'}$ and 4:$(11\bar{1})[\bar{2}1\bar{1}]_{B19'}$ corresponding to {110}<110>$_{B2}$ and other weak components close to χ = 45º associated with variants 2:$(10\bar{2})[211]_{B19'}$, 4:$(10\bar{2})[\bar{2}1\bar{1}]_{B19'}$ and 6:$(10\bar{2})[0\bar{2}0]_{B19'}$ corresponding to {111}<110>$_{B2}$.
- HT+CR+HT condition (Figure 4f) for B2: strong central components associated with the texture component (110)[110]$_{B2}$ and other weak components close to χ = 45º associated with the texture components {001}<110>$_{B2}$.

For all SE alloy conditions (AR – Figure 5a, HT – Figure 5b, and HT+CR+HT – Figure 5c), it is observed texture components close to χ = 18º associated with texture components {210}<110>$_{B2}$ and other components close to χ = 30º associated with texture components {211}<110>$_{B2}$, with RD in <110>.

5 SUMMARY

For the Ni-Ti alloys under study, the heat treatment at 500ºC associated with marforming (30% thickness reduction) is more effective to promote changes in the Ti-rich alloy than in the Ni-rich alloy:

- Resulting in a completely recrystallized structure.
- Inducing the direct and reverse transformation in one step (B2↔B19').
- Promoting the development of the texture component associated to {111}<110>$_{B2}$.
-

Acknowledgments

A.S.P., J.P.H.G.C., K.K.M. and F.M.B.F. acknowledge FCT/MCTES for the pluriannual funding of CENIMAT. C.M.L.S and C.S.C.V acknowledge CNPq (Grant 141664/2002-9) Brazilian agency.

REFERENCES

1 WASILEWSKI, R.J., BUTLER, S.R., HANLON, J.E., WORDEN, D. Homogeneity Range and Martensitic Transformation in TiNi, Metallurgical Transaction, v. 2, p. 229, 1971.

2 KHACHIN, V.N., PASKAL YU, I., GUNTER, V.E., MONASEVICH, A.A., SIVOKHA, V.P. , Fizika Metallov i Metallovedenie, v. 46, p. 511-520, 1978.

3 LIU, Y., CHEN, X., McCORMICK, P.G. Effect of Low Temperature Ageing on the Transformation Behaviour of Near-equiatomic NiTi, Journal of Material Science, v. 32, p. 5979-5984, 1997.

4 SOMSEN, Ch., ZÄHRES, H., KÄSTNER, J., WASSERMANN, E.F., KAKESHITA, T., SABURI, T. Influence of Thermal Annealing on the Martensitic Transitions in Ni-Ti Shape Memory Alloys, Material Science and Engineering A, v. 273-275, p. 310-314, 1999.

5 MILLER, D.A., LAGOUDAS, D.C. Influence of Cold Work and Heat Treatment on the Shape Memory Effect and Plastic Strain Development of NiTi, Material Science and Engineering A, v. 308, p. 161-175, 2001.

6 FILIP, P., MAZANEC, K. On Precipitation Kinetics in TiNi Shape Memory Alloys, Scripta Materialia, v. 45, p. 701-707, 2001.

7 SITEPU, H., SCHMAHL, W.W., VON DREELE, R.B. Quantitative Texture Analysis of Polycrystalline Shape-Memory Alloy NiTi Neutron Diffraction Data by Rietveld Refinement using the Generalized Spherical-Harmonic Description, Shape Memory Materials and their Applications, v. 394-395, p. 233-236, 2002.

8 GORYCZKA, T., MORAWIEC, H. Structure Studies of the R-phase Using X-ray Diffraction Methods, Journal of Alloys and Compounds, v. 367, p. 137-141, 2004.

9 KITAMURA, K., MIYAZAKI, S., IWAI, H., KOHL, M. Effect of Heat-treatment on the Texture in Rolled Ti-Ni Thin Plates, SMST-97: Proceedings of the Second International Conference on Shape Memory and Superelastic Technologies, p. 47-52, 1997.

10 MIYAZAKI, S., OTSUKA, K., WAYMAN, C.M. The Shape Memory Mechanism Associated with the Martensitic Transformation in Ti-Ni Alloys – I. Self-Accommodation, Acta Metallurgica, v. 37, p. 1873-1884, 1989.

11 BRAZ FERNANDES, F.M., PAULA, A.S., CANEJO, J.P.H.G., MAHESH, K.K., SILVA, R.J.C. Kinetics Characterization of Martensitic Transformation on Ti-Rich Ni-Ti SMA, SMST2004: International Conference on Shape Memory and Superelastic Technologies, p. 51-56, 2004.

12 PAULA, A.S., CANEJO, J.P.H.G., MARTINS, R.M.S., BRAZ FERNANDES, F.M. Effect of Thermal Cycling on the Transformation Temperature Ranges of a Ni-Ti Shape Memory Alloy, Material Science and Engineering A, v. 378, p. 92-98, 2004.

13 CANEJO, J.P.H.G. Tratamento Térmico de Ligas com Memória de Forma Visando a Obtenção de Diferentes Gamas de Temperaturas de Transformação, M.Sc. Thesis, FCT/UNL, Lisbon – Portugal, 2005.

14 ZHAO, L. Texture Development and Anisotropic Behaviour in a Ti-45Ni-5Cu (at.%) Shape Memory Alloy, PhD Thesis, Universtiy Twente, The Netherlands, 1997.

15 BHATTACHARYA, T., KOHN, R.V. Symmetry, Texture and the Recoverable Strain of Shape-Memory Polycrystals, Symmetry, Acta Materialia, v. 44, p. 529-542, 1996.

16 SHU, Y.C., BHATTACHARYA, K. The Influence of Texture on the Shape-Memory Effect in Polycrystals, Acta Materialia, v. 46, p.5457-5473, 1998.
17 PAULA, A.S. Tratamentos Termomecânicos de Ligas do Sistema Ni-Ti: Caracterização Estrutural e Optimização das Propriedades Associadas ao Efeito de Memória de Forma, PhD Thesis, FCT/UNL, Lisbon – Portugal, 2006.
18 SANTOS, C.M.L. Ligas Ni-Ti ricas em Ni: Tratamento Térmico, Termomecânico e Efeito de Micromemória de Forma, PhD Thesis, IME, Rio de Janeiro – Brazil, 2006.